Int. J. Therm. Sci. (2001) 40, 289–295

S1290-0729(00)01210-2/FLA

Radiation effects on free convection over a vertical flat plate embedded in a porous medium with high porosity

Md. Anwar Hossain [a]*, Ioan Pop [b]

[a] *Department of Mathematics, University of Dhaka, Dhaka 1000, Bangladesh*
[b] *Faculty of Mathematics, University of Cluj, Cluj, Romania*

(Received 21 February 2000, accepted 11 May 2000)

Abstract — Free convection of an optically thin dense fluid along an isothermal vertical surface embedded in a porous medium with high porosity has been studied. With appropriate transformations the boundary layer equations are reduced to local nonsimilarity equations. Numerical solutions of these equations are obtained by using the Keller box scheme as well as the local nonsimilarity method with second order truncation. The nonsimilar equations governing the flow are simulated by the above methods for fluid of Prandtl number equal to 5.4. Also, effects of the pertinent parameters, R_d, the radiation–conduction parameter and Δ, the surface heating parameter and also the modified Grashof number, Gr^*, on the local skin friction and the local rate of heat transfer are shown graphically. © 2001 Éditions scientifiques et médicales Elsevier SAS

free convection / radiation / porous medium / boundary layer

Nomenclature

a	Rosseland mean absorption coefficient	
f	transformed stream function	
Gr	Grashof number $= g\beta_T(T_w - T_\infty)l^3/\nu^2$	
g	acceleration due to gravity	$m \cdot s^{-2}$
k	thermal conductivity	$W \cdot m^{-1} \cdot K^{-1}$
K	permeability	m^2
K^*	inertial coefficient	
L	reference length	m
Pr	Prandtl number	
q_r	radiation heat flux	$W \cdot m^{-2}$
R_d	conduction–radiation parameter or Planck number	
T	temperature in the boundary layer	K
T_w	constant temperature at the surface	K
T_∞	ambient constant temperature	K
u, v	reference velocity component in the x and y directions	$m \cdot s^{-1}$
x	dimensionless distance measured along the plate	m
y	dimensionless distance normal to the plate	m

Greek symbols

α	equivalent thermal diffusivity	$m^2 \cdot s^{-1}$
β	thermal expansion coefficient	K^{-1}
ϕ	dimensionless pressure function	
η	pseudosimilarity variable	
ν	fluid kinematic viscosity	$m^2 \cdot s^{-1}$
θ	dimensionless temperature function	
θ_w	surface temperature parameter	
ρ	density of the fluid	$kg \cdot m^{-3}$
σ	Stefan–Boltzman constant	$W \cdot m^{-2} \cdot K^{-4}$
σ_s	scattering coefficient	
ψ	stream function	$m^2 \cdot s^{-1}$
ε	porosity of a medium	
γ	Darcy resistance defined in equation (10)	
λ	inertia resistance defined in equation (10)	

1. INTRODUCTION

Free convection in laminar boundary layer flow has been analyzed extensively for semi-infinite flat plates in vertical, horizontal, and inclined orientations. Typical studies can be found in the works of Ostrach [1], Pera and Gebhart [2], Hasan and Eichhorn [3], and Chen and

* Correspondence and reprints.
E-mail address: anwar@du.bangla.net (Md.A. Hossain).

Tzuoo [4]. An excellent review of this problem can be found in the book of Gebhart [5]. On the other hand, heat transfer by simultaneous natural convection and thermal radiation in a participating fluid has not received much attention. However, such study is required because thermal radiation plays a significant role in the overall surface heat transfer in a situation where convective heat transfer coefficients are small, as is the case of natural convection confined to the case of vertical semi-infinite plate; see, for example, Arpaci [6], Cheng and Ozisik [7], Hasegawa et al. [8], Bankston et al. [9], Sparrow and Cess [10], Cess [11] and Ali et al. [12] who first investigated the boundary layer flow over a semi-infinite horizontal plate considering gray-gas that emits and absorbs but does not scatter thermal radiation. However, Hossain and Takhar [13] have recently analyzed the effect of radiation on mixed convection flow of optically thick viscous and incompressible fluid over an isothermal vertical flat plate taking into account the Rosseland diffusion approximation (Siegel and Howell [14]). Using a group of transformations, the boundary layer equations governing the flow were reduced to local nonsimilarity equations, which are valid both in the forced convection and free convection regimes. The resulting equations were solved using the implicit finite difference method together with Keller box elimination scheme (Cebeci and Bradshaw [15]). It should further be mentioned that the problem of natural convection with conduction–radiation effects on the flow along a thin vertical cylinder has recently been investigated by Hossain and Alim [16].

Although convective flow in porous media has been widely studied in the recent years (see Nield and Bijan [17]) and Ingham and Pop [18]), the effect of thermal radiation with Rosseland diffusion approximation on the free convection boundary layer flow of an optically dense viscous incompressible fluid along a heated vertical flat plate which is embedded in fluid-saturated porous medium with high porosity has not, as the authors are aware, yet been studied. Therefore, the present paper proposes to investigate the effects of radiation on free convection boundary layer flow of an optically dense viscous incompressible fluid from a vertical plate immersed in a porous medium of high porosity using Froschheimer–Darcy flow model. Employing the appropriate transformation, governing boundary layer equations are transformed to local nonsimilarity equations. This set of equations is then solved numerically using the Keller box method as well as the local nonsimilarity method (Minkowycz and Sparrow [19, 20]) taking the second level of truncation in consideration. Solutions are obtained for a high porous medium, for which $\varepsilon = 1$, and a wide ranged values of radiation parameter R_d and the surface temperature parameter Δ. The present investigations have been made only for the fluid having a Prandtl number Pr of 5.4. Results are presented graphically for local skin friction coefficient and local Nusselt number as well as the velocity and temperature distributions.

2. MATHEMATICAL FORMULATION

Consider the steady two-dimensional free convection boundary layer flow of an optically dense viscous and incompressible fluid over a vertical plate embedded in a porous medium of high porosity as shown in *figure 1*. We assume that the plate is heated to a constant temperature, T_w, which is higher than that the temperature, T_∞, of the ambient fluid-saturated porous medium. In order to study transport through high porosity media, the original model of Darcy was improved by including the boundary and inertia effects using volume averaged principals by Vafai and Tien [21]. In addition, the following assumptions are maid for the formulation: the fluid and porous medium are everywhere in local thermodynamic equilibrium; the porous medium is isotropic and homogeneous; properties of the fluid and the porous medium such as viscosity, thermal conductivity, thermal expansion coefficient and permeability are constant. Under these assumptions the boundary layer equations governing the flow become

$$\frac{\partial \bar{u}}{\partial \bar{x}} + \frac{\partial \bar{v}}{\partial \bar{y}} = 0 \tag{1}$$

$$\frac{1}{\varepsilon^2}\left(\bar{u}\frac{\partial \bar{u}}{\partial \bar{x}} + \bar{v}\frac{\partial \bar{u}}{\partial \bar{y}}\right) = g\beta(T - T_\infty) + \frac{\nu}{\varepsilon}\left(\frac{\partial^2 \bar{u}}{\partial \bar{y}^2} - \frac{\varepsilon}{K}\bar{u} - \varepsilon K^* \bar{u}^2\right) \tag{2}$$

$$\bar{u}\frac{\partial T}{\partial \bar{x}} + \bar{v}\frac{\partial T}{\partial \bar{y}} = \alpha\left(\frac{\partial^2 T}{\partial \bar{y}^2} - \frac{1}{k}\frac{\partial q_\mathrm{r}}{\partial \bar{y}}\right) \tag{3}$$

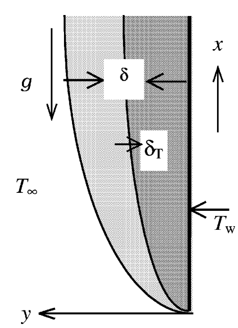

Figure 1. The flow configuration and the coordinate system. δ_M and δ_T are respectively the momentum and thermal boundary layer thickness.

where $\bar{u}$, $\bar{v}$ are the velocity components in the $\bar{x}$, $\bar{y}$ direction; T is the fluid temperature, K is the permeability, K^* is a measure of the inertia impedance of the matrix (Ergun [22]), ε is the porosity, k is the thermal conductivity, α is the equivalent thermal diffusivity, β is the thermal expansion coefficient, g is the acceleration due to gravity and q_r is the radiative heat flux in the $\bar{y}$ direction. In order to reduce the complexity of the problem and to provide a means of comparison with future studies that will employ a more detailed representation for the radiative heat flux, we will consider the optically thick radiation limit. Thus, radiation heat flux term is simplified by the Rosseland diffusion approximation proposed by Siegel and Howell [14] and is given as

$$q_r = -\frac{4\sigma}{3k(a+\sigma_s)}\frac{\partial T^4}{\partial \bar{y}} \tag{4}$$

where σ is the Stefan–Boltzman constant and σ_s is the scattering coefficient. Relation (4) is valid only for intensive absorption.

In the momentum equation (2), for low porosity media, the convective term and the viscous term are responsible for boundary effects, which are very small and can be neglected (see Chen and Minkowycz [23]). On the other hand, for a high porosity media the boundary and convective effects are important, especially at the upstream end of the heated plate.

The boundary conditions to be satisfied are

$$\begin{aligned} &\bar{y}=0: && \bar{u}=\bar{v}=0, \quad T=T_w \\ &\bar{y}\to\infty: && \bar{u}\to 0, \qquad T\to T_\infty \end{aligned} \tag{5}$$

Introducing the new variables

$$\begin{aligned} &\bar{u}=\frac{\nu}{L}Gr^{1/2}u, \qquad \bar{v}=\frac{\nu}{L}Gr^{-1/4}v \\ &\theta=\frac{T-T_\infty}{T_w-T_\infty} \\ &x=\frac{\bar{x}}{L}, \qquad y=\frac{\bar{y}}{L}Gr^{1/4} \end{aligned} \tag{6}$$

where $Gr = g\beta(T_w - T_\infty)L^3/\nu^2$ is the Grashof number, equations (1)–(3) become

$$\frac{\partial u}{\partial x}+\frac{\partial v}{\partial y}=0 \tag{7}$$

$$\frac{1}{\varepsilon^2}\left(u\frac{\partial u}{\partial x}+v\frac{\partial u}{\partial y}\right)=\theta+\frac{1}{\varepsilon}\left(\frac{\partial^2 u}{\partial y^2}-\varepsilon\gamma u-\lambda u^2\right) \tag{8}$$

$$u\frac{\partial\theta}{\partial\bar{x}}+v\frac{\partial\theta}{\partial\bar{y}}=\frac{1}{Pr}\frac{\partial}{\partial y}\left[\left\{1+\frac{4}{3}R_d(1+\Delta\theta)^3\right\}\frac{\partial\theta}{\partial y}\right] \tag{9}$$

where $Pr = \nu/\alpha$ is the Prandtl number. Other parameters are defined as follows:

$$\begin{aligned} &\gamma=\frac{1}{Gr_L^{1/2}Da_L}, \qquad Da_L=\frac{L^2}{K}, \qquad \lambda=LC \\ &R_d=\frac{4\sigma T_\infty^3}{3\kappa(a+\sigma_s)} \quad \text{and} \quad \Delta=\frac{T_w}{T_\infty}-1 \end{aligned} \tag{10}$$

Here γ is the Darcy resistance parameter, Da_L the Darcy number, λ the inertia resistance, R_d the Planck constant or the conduction–radiation parameter and Δ the surface temperature parameter. Here we consider that the surface is heated for which Δ is positive (i.e. when $T_w/T_\infty > 1$).

The boundary conditions (5) then become

$$\begin{aligned} &u=v=0,\ \theta=1 && \text{at } \eta=0 \\ &u,\theta\to 0 && \text{as } \eta\to\infty \end{aligned} \tag{11}$$

We now introduce the following new variables:

$$\begin{aligned} &\psi=(4x)^{3/4}f(\eta,\xi), \qquad \eta=\frac{y}{(4x)^{1/4}} \\ &\theta=\theta(\eta,\xi), \qquad \xi=2\gamma x^{1/2} \end{aligned} \tag{12}$$

where ξ is the termed as the Darcy parameter, η is the pseudo-similarity variable and ψ is the stream function, which is defined in the usual way as

$$u=\frac{\partial\psi}{\partial y} \quad \text{and} \quad v=-\frac{\partial\psi}{\partial x} \tag{13}$$

Using (12) in (13), we thus have

$$u=4Gr_L^2Da_L\xi f'(\eta,\xi) \tag{14}$$

$$v=\left(4Gr_LDa_L^2\right)^{-1/4}(2\xi)^{-1/2}\left[3f-\eta f'+2\xi\frac{\partial f}{\partial\xi}\right] \tag{15}$$

so that equations (8) and (9) become

$$\begin{aligned} &\frac{1}{\varepsilon}f'''+\frac{1}{\varepsilon^2}\left(3ff''-2f'^2\right)+\theta-\xi\left(f'+Gr^*f'^2\right) \\ &\quad=\frac{2\xi}{\varepsilon^2}\left(f'\frac{\partial f'}{\partial\xi}-f''\frac{\partial f}{\partial\xi}\right) \end{aligned} \tag{16}$$

$$\begin{aligned} &\frac{1}{Pr}\left[\left\{1+\frac{4}{3}R_d(1+\Delta\theta)^3\right\}\theta'\right]'+3f\theta' \\ &\quad=2\xi\left(f'\frac{\partial\theta}{\partial\xi}-\theta'\frac{\partial f}{\partial\xi}\right) \end{aligned} \tag{17}$$

In equation (16), $Gr^* = \beta(T_w - T_\infty)KK^*/\nu^2$ is the modified Grashof number for porous media and primes denote the differentiation with respect to η. We notice that if Gr^* is very small inertia effects can be neglected. This may be true for low-porosity media, such as foam materials; Gr^* can also be very large and inertia effects are then very significant (Vafai and Tien [21]).

In the situation where the wall temperature T_w is not very much different from the ambient temperature T_∞, equation (17) can be approximated by

$$\frac{1}{Pr}\left(1+\frac{4}{3}R_d\right)\theta''+3f\theta'=2\xi\left(f'\theta_\xi-\theta' f_\xi\right) \tag{18}$$

The corresponding boundary conditions take the form

$$\begin{aligned} &f(\xi,0)=f'(\xi,0)=0, \qquad \theta(\xi,0)=1 \\ &f'(\xi,\infty)=\theta(\xi,\infty)=0 \end{aligned} \tag{19}$$

where primes denote differentiation of the functions with respect to η.

3. NUMERICAL METHOD

The present problem in the absence of radiation effect has been investigated by Hong et al. [24]. In investigating the present problem the authors propose to employ only two methods, namely, the Keller box method and the local nonsimilarity method.

3.1. Keller box method

A very efficient and accurate implicit finite difference method (the Keller box method) will be employed here to solve the nonlinear system of partial differential equations (16) and (17). To do this, equations (16) and (17) are written in terms of a system of first-order equations in η, which is then expressed in finite difference form by approximating the functions and their derivatives in terms of the central differences in both coordinate directions. Denoting the mesh points in the (ξ,η) plane by ξ_i and η_j, where $i=1,2,3,\ldots,M$ and $j=1,2,3,\ldots,N$, central difference approximations are made such that the equations involving ξ explicitly are centered at $(\xi_{i-1/2},\eta_{j-1/2})$ and the remainder at $(\xi_i,\eta_{j-1/2})$, where $\eta_{j-1/2}=\eta_j+\eta_{j-1}$, etc. This results in a set of nonlinear difference equations for the unknowns at ξ_j in terms of their values at ξ_{i-1}. These equations are then linearized by Newton's quasi-linearization technique and solved using a block-tridiagonal algorithm, taking as the initial iteration the converged solution at $\xi=\xi_{i-1}$. Now to initiate the process at $\xi=0$, we first provide guess profiles for all five variables (arising from the reduction to the first-order form) and use the Keller box method to solve the governing ordinary differential equations. Having obtained the leading-edge solution it is possible to march step by step along the boundary layer. For a given value of ξ, the iterative procedure is stopped when the difference in computing the velocity and the temperature in the next iteration is less than 10^{-6}, i.e. when $|\delta f^i|\le 10^{-6}$, where the superscript i denotes the iteration number. The computations were not performed using a uniform grid in the η direction, but a non-uniform grid was used and defined by $\eta_j=\sinh((j-1)/a)$, with $j=1,2,\ldots,251$ and $a=100$. The η_j values were chosen so that the outer boundary $\eta_e\approx 8$, which is sufficiently large, and they are such that the grid is sufficiently dense in the vicinity of the boundary to ensure accuracy; this is important because the boundary layer thins substantially as ξ increases, as shown in the asymptotic solution above. In the present numerical investigation the maximum values of ξ were chosen to be sufficiently large that the solutions compare well with the asymptotic values for the local skin friction and the local rate of heat transfer. The numerical results thus obtained are shown graphically and in tabular form.

Once we know the values of $f(\eta,\xi)$, $\theta(\eta,\xi)$ and their derivatives one can calculate the values of the local skin friction and the local rate of heat transfer at the surface from the following relations:

$$C_{fx}Gr_x^{1/4}=f''(0,x) \tag{20}$$

and

$$\frac{Nu_x}{Gr_x^{1/4}}=-\left\{1+\frac{4}{3}R_d(1+\Delta)^3\right\}\theta'(0,x) \tag{21}$$

3.2. Local nonsimilarity method

We now discuss the local nonsimilarity method to solve equations (16) and (17). Since it was already seen in papers of Minkowycz and Sparrow [19, 20] that for the problem of coupled local nonsimilarity equations, consideration of equation up to the second level of truncation gives almost accurate results comparable with the solutions from other methods such as finite difference method, we will consider here the local nonsimilar equations (16) and (17) only up to the second level of truncation. To do this, we introduce the following new functions:

$$g=\frac{\partial f}{\partial\xi},\qquad \phi=\frac{\partial\theta}{\partial\xi} \tag{22}$$

Introducing these functions into (17) and (18) we get

$$\frac{1}{\varepsilon}f''' + \frac{1}{\varepsilon^2}\left(3ff'' - 2f'^2\right) + \theta - \xi\left(f' + Gr^*\xi f'^2\right) = \frac{2\xi}{\varepsilon^2}\left(f'g' - f''g\right) \quad (23)$$

$$\frac{1}{Pr}\left[\left\{1 + \frac{4}{3}R_d(1+\Delta\theta)^3\right\}\theta'\right]' + 3f\theta' = 2\xi\left(f'\phi - \theta' g\right) \quad (24)$$

Differentiating the above equations with respect to ξ one may easily find by neglecting the terms involving the derivative functions of g and ϕ with respect to ξ as follows:

$$\frac{1}{\varepsilon}g''' + \frac{1}{\varepsilon^2}\left(3fg'' + 5f''g - 6f'g'\right) + \phi - \left(f' + \xi g'\right) - 2Gr^*\xi\left(f'^2 + \xi f'g'\right) = \frac{2\xi}{\varepsilon^2}\left(g'^2 - gg''\right) \quad (25)$$

$$\frac{1}{Pr}\left[\left\{1 + \frac{4}{3}R_d(1+\Delta\theta)^3\right\}\phi'' + 4\Delta R_d(1+\Delta\theta)^2\left(2\theta'\phi' + \theta''\phi\right) + 8\Delta^2 R_d(1+\Delta\theta)\theta'^2\phi\right] + 3f\phi' + 5\theta' g - 2f'\phi = 2\xi\left(g'\phi - g\phi'\right) \quad (26)$$

The appropriate boundary conditions to be satisfied by the above equations are

$$\begin{aligned} &f(0,\xi) = f'(0,\xi) = 0, \qquad \theta(0,\xi) = 1 \\ &f'(\infty,\xi) = \theta(\infty,\xi) = 0 \\ &g(0,\xi) = g'(0,\xi) = \phi(0,\xi) = 0 \\ &g'(\infty,\xi) = \phi(\infty,\xi) = 0 \end{aligned} \quad (27)$$

4. RESULTS AND DISCUSSIONS

The numerical results for skin friction and the Nusselt number are obtained for representative values of the Planck number R_d and surface temperature parameters θ_w against the local Darcy parameter ξ. It should be noted here that for both CO_2 in the temperature range 100–650 °F (with the corresponding Prandtl number range 0.76–0.6) and NH_3 vapor in the temperature range 120–400 °F (with the corresponding Prandtl number range 0.88–0.84) at 1 atm, the value of R_d ranges approximately from 0.033 to 0.1, whereas for water vapor in the temperature range 220–900 °F (with the corresponding Prandtl number $Pr \approx 1.0$) the R_d values lie between 0.02 and 0.3.

Here we present results obtained by using two distinct solution techniques, namely, the Keller box method and the local nonsimilarity method for flow with high porosity media, i.e. $\varepsilon = 1$. Values of the other parameters are $R_d = 0.0$, 1.0, 2.0, 3.0 and 4.0, $Gr^* = 0.0$, 1.0 and 2.0, $\Delta = 0.1$ and $Pr = 5.4$.

In *table I* we first entered the numerical values of the local skin friction coefficient, $C_{fx}/Gr_x^{1/4}$, and the local Nusselt number, $Nu_x/Gr_x^{1/4}$, obtained from the Keller box solutions and the local nonsimilarity solutions for values of the surface temperature parameter $\Delta = 0.1$ and 1.0 against ξ in $[0, 3]$, taking $R_d = 1.0$ and 4.0, $Gr^* = 1.0$. Comparisons between the two solutions are found in excellent agreement. Maximum difference between these solutions, in respect to $C_{fx}/Gr_x^{1/4}$ and $Nu_x/Gr_x^{1/4}$, is found to be 0.02 % for both the values of $\Delta = 0.1$ and 1.0. From this table we further notice that increase in the value of the surface temperature leads to rise in the value of the skin friction coefficient and a fall in the value of the local Nusselt number.

The variation of the skin friction coefficient $C_{fx}/Gr_x^{1/4}$ and the local Nusselt number $Nu_x/Gr_x^{1/4}$ with ξ is shown in *figures 2* and *3*. Here also we notice that the agreement between the results obtained by using the Keller box method and local nonsimilarity technique is very good. Then, it can be seen that an increase of the conduction–radiation parameter R_d leads to an increase in the skin friction coefficient and to a decrease in the local Nusselt number. This may be attributed to the fact that the increase of the values of R_d implies more interaction of radiation with the momentum boundary layer and less interaction with the thermal boundary layer. These figures also show that both the skin friction coefficient

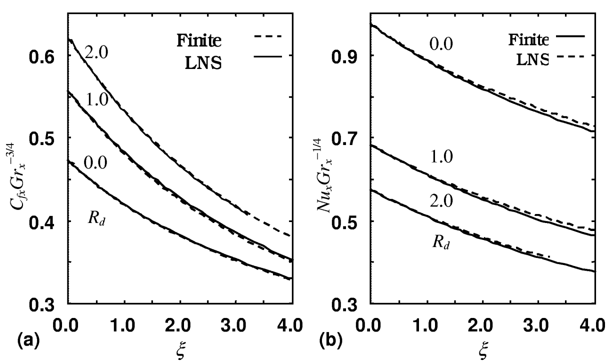

Figure 2. (a) Skin friction coefficient and (b) Nusselt number coefficient against ξ for different values of $R_d = 0.0$, 1.0 and 2.0 while $Pr = 5.4$, $\Delta = 01.1$, and $Gr^* = 1.0$.

TABLE I
Numerical values of the local skin friction and local Nusselt number for $Pr = 5.4$, $Gr = 1.00$, $R_d = 1.00$ and $\Delta = 0.1$ and 1.0.

	$C_{fx}Gr_x^{-3/4}$		$Nu_xGr_x^{-1/4}$		$C_{fx}Gr_x^{-3/4}$		$Nu_xGr_x^{-1/4}$	
Δ	1.1	2.0	1.1	2.0	1.0	2.0	1.0	2.0
ξ	Finite difference method				Local nonsimilarity method			
0.0	0.5657	0.6920	0.6822	0.3233	0.5651	0.6909	0.6822	0.3235
0.1	0.5575	0.6811	0.6748	0.3197	0.5572	0.6801	0.6749	0.3200
0.2	0.5494	0.6701	0.6673	0.3160	0.5492	0.6693	0.6676	0.3164
0.3	0.5414	0.6591	0.6598	0.3123	0.5413	0.6584	0.6603	0.3128
0.4	0.5336	0.6481	0.6524	0.3086	0.5336	0.6475	0.6530	0.3091
0.5	0.5259	0.6372	0.6450	0.3048	0.5259	0.6366	0.6458	0.3054
0.6	0.5184	0.6265	0.6377	0.3009	0.5183	0.6258	0.6386	0.3017
0.7	0.5110	0.6158	0.6304	0.2971	0.5109	0.6151	0.6316	0.2981
0.8	0.5039	0.6054	0.6232	0.2933	0.5036	0.6044	0.6246	0.2944
0.9	0.4969	0.5951	0.6161	0.2894	0.4965	0.5940	0.6178	0.2908
1.0	0.4900	0.5850	0.6091	0.2856	0.4896	0.5836	0.6111	0.2873
1.5	0.4585	0.5380	0.5759	0.2671	0.4575	0.5348	0.5796	0.2715
2.0	0.4312	0.4973	0.5459	0.2500	0.4296	0.4918	0.5518	0.2604
2.5	0.4075	0.4625	0.5191	0.2347	0.4055	0.4566	0.5278	0.2524
3.0	0.3868	0.4331	0.4952	0.2214	0.3845	0.4286	0.5069	0.2386

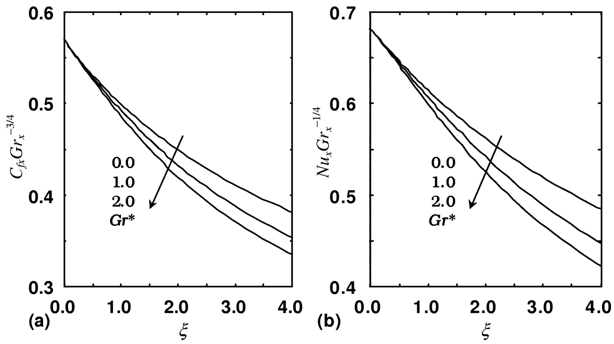

Figure 3. (a) Skin friction coefficient and (b) Nusselt number coefficient against ξ for different values of $Gr^* = 0.0$, 1.0, 2.0 while $Pr = 5.4$, $\Delta = 0.1$, and $R_d = 1.0$.

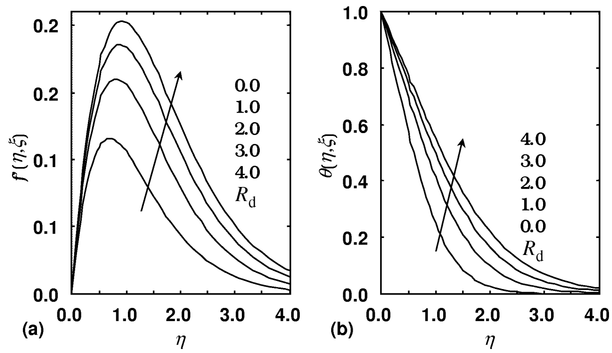

Figure 5. (a) Velocity profile and (b) temperature profile for values of $R_d = 0.0$, 1.0, 2.0, 3.0 and 4.0 while $Pr = 5.4$, $Gr^* = 1.0$, $\Delta = 0.1$ at $\xi = 1.0$.

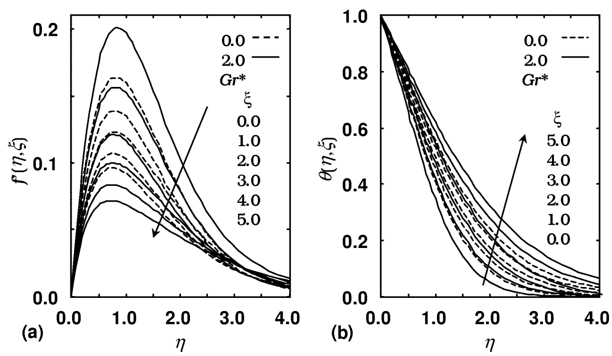

Figure 4. (a) Velocity profile and (b) temperature profile for values of $\xi = 0.0$, 1.0, 2.0, 3.0 and 4.0 while $Pr = 5.4$, $\Delta = 0.1$, $R_d = 1.0$ and $Gr^* = 0.0$, 2.0.

and the local Nusselt number decrease with the increase of the modified Grashof number Gr^*.

The influence of the parameters ξ, Gr^* and R_d on the reduced velocity and temperature fields is illustrated in *figures 4* and *5*. From *figure 4* we can see that the velocity profiles decrease with the increase of ξ, while the nondimensional temperature profiles increase with the increase of ξ. Further, *figure 5* shows that the velocity profiles increase with the increase of the parameter, while the nondimensional temperature profiles increase with the increase of R_d. This is in agreement with the results shown in *figure 2*.

5. CONCLUSIONS

The interaction of thermal radiation with the free convection boundary layer flow of an optically dense fluid over a vertical surface embedded in a porous medium of high porosity using the Brinkman–Forchheimer–Darcy extended model. Two distinct techniques, namely, the Keller box method and the local nonsimilarity scheme, have been used to solve numerically the transformed governing equations. Calculations were carried out for a wide range of values of the pertinent parameters to examine the results from these methods. It has been found that the skin friction coefficient and the local rate of heat transfer predicted by these methods are in very good agreement. It has also been seen that the influence of the thermal radiation parameter as well as the surface temperature is to rise the value of the local skin friction coefficient and to reduce the value of the local Nusselt number.

REFERENCES

[1] Ostrach S., An analysis of laminar free convection flow and heat transfer about a flat plate parallel to the direction of the generating body force, NACA TN 2635, 1952.

[2] Pera L., Gebhart B., Natural convection boundary layer over horizontal and slightly inclined surfaces, Int. J. Heat Mass Tran. 16 (1973) 1131–1146.

[3] Chen T.S., Tzuoo K.L., Vortex instability of free convection flow over plate, ASME J. Heat Tran. 101 (1979) 642–647.

[4] Hasan M.M., Eichorn R., Local nonsimilarity solution of free convection flow and heat transfer from horizontal and inclined surfaces, ASME J. Heat Tran. 104 (1982) 637–643.

[5] Gebhart B., Jaluria Y., Mahajan R.L., Samakia B., Buoyancy-Induced Flow and Transport, Hemisphere, New York, 1988.

[6] Arpaci V.S., Effect of thermal radiation on the laminar free convection from a heated vertical plate, Int. J. Heat Mass Tran. 11 (1968) 871–881.

[7] Cheng E.H., Ozisik M.N., Radiation with free convection in an absorbing, emitting and scattering medium, Int. J. Heat Mass Tran. 15 (1972) 1243–1252.

[8] Hasegawa S., Echigo R., Fakuda K., Analytic and experimental studies on simultaneous radiative and free convective heat transfer along a vertical plate, Proc. Japanese Soc. Mech. Engineers 38 (1972) 2873–2883 and 39 (1973) 250–257.

[9] Bankston J.D., Lloyd J.R., Novonty J.L., Radiation convection interaction in an absorbing-emitting liquid in natural convection boundary layer flow, ASME J. Heat Tran. 99 (1977) 125–127.

[10] Sparrow E.M., Cess R.D., Radiation Heat Transfer, augmented edition, Hemisphere, Washington, DC, 1978, chapters 7, 10.

[11] Chess R.D., Interaction of thermal radiation with free convection heat transfer, ASME J. Heat Tran. 104 (1982) 637–647.

[12] Ali M.M., Chen T.S., Armaly B.F., Natural convection-radiation interaction in boundary layer flow over horizontal surface, AIAA J. 22 (1984) 1797–1803.

[13] Hossain M.A., Takhar H.S., Radiation effect on mixed convection along a vertical plate with uniform surface temperature, Heat Mass Tran. 31 (1996) 243–248.

[14] Siegel R., Howell J.R., Thermal Radiation Heat Transfer, McGraw-Hill, New York, 1972.

[15] Cebeci T., Bradshaw P., Physical and Computational Aspects of Convective Heat Transfer, Springer, New York, 1984.

[16] Hossain M.A., Alim M.A., Natural convection–radiation interaction on boundary layer flow along a thin vertical cylinder, Heat Mass Tran. 32 (1997) 515–520.

[17] Nield D.A., Bejan A., Convection in Porous Media, 2nd edition, Springer, New York, 1999.

[18] Ingham D.B., Pop I. (Eds.), Transport Phenomena in Porous Media, Pergamon, Oxford, 1998.

[19] Minkowycz W.J., Sparrow E.M., Numerical solution scheme for local nonsimilarity boundary-layer analysis, Numer. Heat Tran. 1 (1978) 69–85.

[20] Minkowycz W.J., Sparrow E.M., Interaction between surface mass transfer and transverse curvature in natural convection boundary layers, Int. J. Heat Mass Tran. 22 (1979) 1445–1454.

[21] Vafai K., Tien C.L., Boundary and inertia effects on flow and heat transfer in porous media, Int. J. Heat Mass Tran. 24 (1981) 195–203.

[22] Ergun S., Fluid flow through packed columns, Chem. Engrg. Proc. 48 (1952) 84–94.

[23] Cheng P., Minkowycz W.J., Free convection about a vertical plate embedded in a porous medium with application to heat transfer from a dike, J. Geophys. Res. 82 (1977) 2040–2044.

[24] Hong J.T., Tien C.L., Kaviany M., Non-Darcy effect on vertical plate natural convection in porous media with high porosity, Int. J. Heat Mass Tran. 28 (1985) 2149–2157.